Available online at www.sciencedirect.com
ScienceDirect
European Journal of Pharmaceutics and Biopharmaceutics 69 (2008) 852–860
European Journal of Pharmaceutics and Biopharmaceutics
www.elsevier.com/locate/ejpb

Research paper

Transport and structural analysis of molecular imprinted hydrogels for controlled drug delivery

Siddarth Venkatesh [a], Jishnu Saha [a], Shondra Pass [a,b], Mark E. Byrne [a,b,*]

[a] *Biomimetic and Biohybrid Materials, Biomedical Devices, and Drug Delivery Laboratories, Department of Chemical Engineering, Auburn University, Auburn, AL, USA*

[b] *NSF REU Program in Micro/Nano-Structured Materials, Therapeutics, and Devices, Auburn University, Auburn, AL, USA*

Received 27 July 2007; accepted in revised form 30 January 2008
Available online 15 February 2008

Abstract

Molecular imprinting provides a rational design strategy for the development of controlled release drug delivery systems. We demonstrate that imprinting a hydrogel network results in macromolecular memory for the template molecule, indicated by the two or more times greater partitioning into these networks as compared to non-imprinted networks. Partitioning of drug into networks synthesized from multiple functional monomers was 8 times greater than networks synthesized from single monomers. One-dimensional permeation studies showed that the gel with maximum incorporated chemical functionality had the lowest diffusion coefficient, which was one to two orders of magnitude lower than all other gels studied. All imprinted networks had significantly lower diffusion coefficients than non-imprinted networks, in spite of comparable mesh sizes and equilibrium polymer volume fractions in the swollen state, which to our knowledge, is the first time that such a study has been conducted in the literature. We propose the "tumbling hypothesis", wherein a molecule tumbling through an imprinted network with multiple, organized functionalities and an appropriate mesh size, experiences heightened interactions with memory sites and shows delayed transport kinetics. Thus, the structural plasticity of polymer chains, i.e. the organization of functional groups into memory sites, may be responsible for enhanced loading and extended release.

Keywords: Drug delivery; Controlled release; Sustained release; Molecular imprinting; Structural plasticity; Macromolecular memory

1. Introduction: Extending therapeutic delivery by hydrogel design

Controlled drug release from hydrogels has been extensively studied for the past three decades. Hydrogels are insoluble, crosslinked polymer network structures composed of hydrophilic homo- or hetero-co-polymers, which have the ability to absorb significant amounts of water and retain their shape without dissolving. Crosslinks (otherwise known as tie-points or junctions) can be covalent bonds, permanent entanglements, ionic interactions, or microcrystalline regions incorporating various chains.

Two schemes are used to load therapeutics into hydrogels – produce the gel in the presence of drug or synthesize the gel and then load drug into the gel via equilibrium partitioning. Previous work from our laboratory has demonstrated that drug included in monomer mixtures can affect polymerization kinetics during network formation [1]. Surprisingly, no work has addressed the potential optimization of extended release properties via tailored drug-functional monomer interactions. This paper presents a novel way to delay therapeutic transport by creating macromolecular memory in the gel, by providing multiple diverse functional groups for extensive non-covalent interactions between the gel and the therapeutic. This could prove to be a valuable tool in the rational design of controlled release hydrogel carriers and significantly increase the applicability of such systems in thin film or 'limited volume' applications.

* Corresponding author. Biomimetic and Biohybrid Materials, Biomedical Devices, and Drug Delivery Laboratories, Department of Chemical Engineering, Auburn University, 212 Ross Hall, Auburn, AL 36849-5127, USA. Tel.: +1 334 844 2862; fax: +1 334 844 2063.
E-mail address: byrneme@eng.auburn.edu (M.E. Byrne).

0939-6411/$ - see front matter © 2008 Elsevier B.V. All rights reserved.
doi:10.1016/j.ejpb.2008.01.036

The value of hydrogels in drug delivery comes from their ability to control the diffusion behavior of molecules in or through them; and the ability to amplify the microscopic events occurring at the mesh chain level into macroscopic phenomena [2,3]. When a dry hydrogel is immersed in a thermodynamically compatible solvent, the solvent movement into the hydrogel polymer chains leads to considerable volume expansion and macromolecular rearrangement depending on the extent of crosslinking within the network (Fig. 1a). The rate at which a polymer expands or swells depends upon two coupled processes, the relative rates of polymer-chain relaxation and solvent penetration into the network. The hydrogel transitions in a moving front from an unperturbed, glassy state to a solvated, rubbery state with an increase in macromolecular mobility due to chain extension, and this leads to additional free-volume for transport. For swelling-controlled hydrogels, if there is a constant rate of solvent front penetration which is much smaller than the drug diffusion rate in the swollen gel, a zero-order release or constant release rate arises.

Typically, drug transport can be controlled by swelling-controlled systems (i.e., drug-loaded dry state with water uptake, gel swelling, and drug release) or swellable systems such as a swollen gel that undergoes a reversible volume transition based on a stimulus (e.g., pH, temperature, ionic strength, biomolecular binding event etc.). Swellable hydrogels can be engineered to be sensitive to environmental conditions due to the presence of specific chemical/biological species along their backbone polymer chains (Fig. 1b).

In a Fickian model of release kinetics, the relaxation rate is high and the diffusion processes are rate-limiting, resulting in the release rate of the drug being proportional to the concentration gradient between the drug source and the surroundings. The challenge is to use a finite drug source to achieve an extended zero-order release, and a number of strategies have been attempted such as bioerodible and biodegradable systems with solvent penetration fronts moving with similar velocities as the outer eroding front [4], hydrogels with rate controlling-barriers such as higher crosslinked outer edges [5], and non-uniform drug distribution [6].

A relatively new method is to exploit molecular imprinting methods which can create macromolecular memory for the drug within the network and delay the transport of drug from the matrix via interaction of the drug with numerous functional groups organized within the network (Fig. 1c). The drug's heightened interaction with the memory pockets slows its release from the hydrogel despite comparable free volume within the polymer chains for drug transport. This type of network formation – with a proper optimization of drug affinity relating to number and strength of functional monomer interactions, crosslinking structure, and mobility of polymer chains – has a strong potential to influence a number of hydrogel carriers and

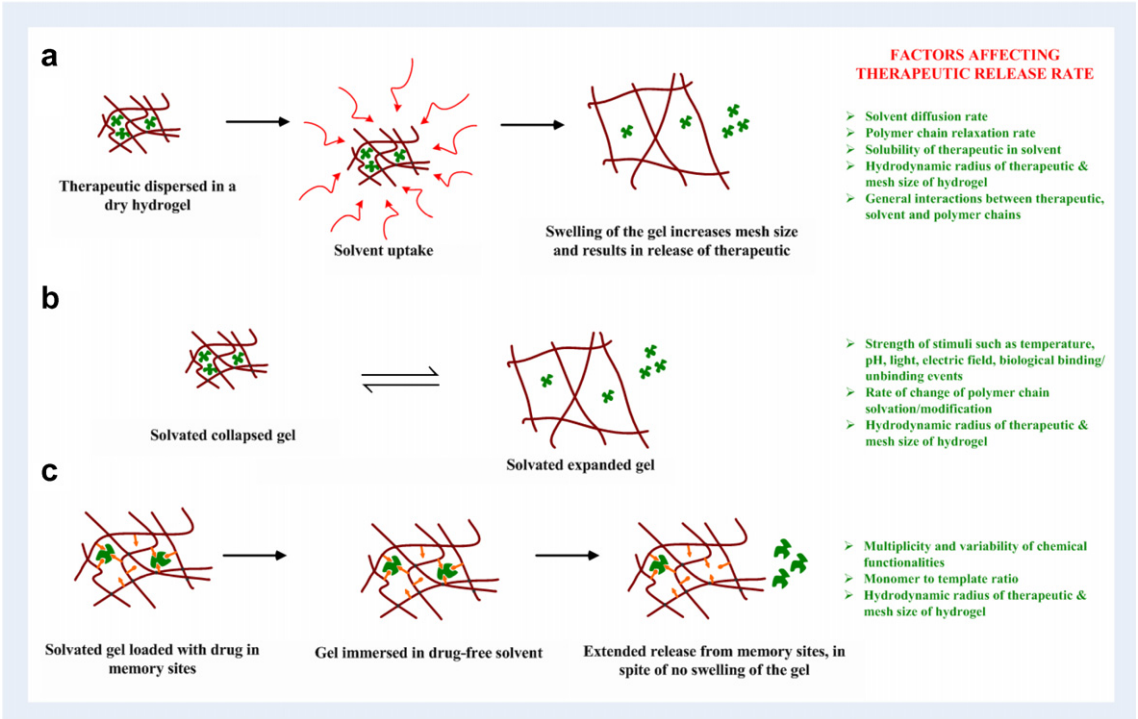

Fig. 1. (a) Controlled drug release in hydrogels hinges upon their swelling either upon solvent uptake from a dry state or (b) thermodynamic compatibility with the solvent. (c) Macromolecular memory obtained by the imprinting of a multifunctional pre-polymerization complex with the drug, is an alternative strategy to release the drug in a controlled fashion when the gels are already solvated and fully swollen.

add to the variables one can alter to tune the release profile. As drug delivery materials decrease in length scales towards nanoparticles and thin films, further control of transport at decreasing thicknesses is paramount for the success of such systems. The additional rational design of hydrogel structures has significant potential in limited volume applications.

2. Use of molecular imprinting techniques to rationally design gel carriers

It is only recently that molecular imprinting strategies have been harnessed in drug delivery. Molecular imprinting is a synthesis technique exploiting template-mediated polymerization mechanisms to produce synthetic macromolecular networks with tailored affinity, capacity, and selectivity for a template molecule. The majority of imprinted systems in drug delivery studied to date include highly crosslinked structures and not weakly crosslinked systems such as hydrogels. In the last few years, there has been increased interest in weakly crosslinked structures, aqueous-based recognition, as well as biologically significant template molecules. We direct the reader to conventional molecular imprinting reviews [7,8], as well as bio-focused and drug delivery reviews [9–11].

Table 1 presents recent studies that analyzed the transport of template (release or loading versus time) from imprinted structures. It is clear that imprinting enhances loading capacity/affinity but the influence of imprinting on the release of therapeutic is much more complex, with little attention in these recent studies to structural analysis. Delayed transport of template could be influenced by differences in macromolecular structure and organization of the network chains, different concentration driving forces, as well as differences in porosity between imprinted and non-imprinted networks. It is also very evident that few studies have been conducted on low or weakly crosslinked imprinted gels.

3. Materials and methods

3.1. Materials and reagents

Acrylic acid (AA), acrylamide (AM), 2-hydroxyethylmethacrylate (HEMA), *N*-vinyl 2-pyrrolidinone (NVP), azobisisobutyronitrile (AIBN) and ketotifen fumarate were purchased from Sigma–Aldrich (Milwaukee, WI). Polyethylene glycol (200) dimethacrylate (PEG200DMA) was purchased from Polysciences, Inc. (Warrington, PA). All chemicals were used as received.

3.2. Synthesis and loading of molecularly imprinted hydrogels

Hydrogels of differing compositions were synthesized in a temperature controlled, non-oxidative environment using UV free-radical photopolymerization as reported earlier [1]. A rigorous analysis of ligand binding was conducted and we chose the functional monomers based on similar specific interactions in biological receptors [12]. These interactions are hydrogen bonds between ketotifen fumarate and the carboxyl side chains of acrylic acid, the amide side chains of acrylamide, and ring interactions with *N*-vinyl pyrrolidinone. Polymer compositions consisted of 5 mole% crosslinking monomer and 95 mole% functional monomer (92 mole% backbone functional monomer, HEMA, and the balance 3 mole% as combinations of other functional monomers). Copolymer networks were made using various combinations of above monomers (e.g., poly(AA-co-HEMA-co-PEG200DMA), poly(AM-co-HEMA-co-PEG200DMA), poly(NVP-co-HEMA-co-PEG200DMA), poly(AA-co-AM-co-HEMA-co-PEG200DMA), and poly (AA-co-AM-co-NVP-co-HEMA-co-PEG200DMA). Control gels were made in exactly the same manner except ketotifen fumarate was not included in the formulation. The hydrogels were cut into discs, washed with deionized water until ketotifen fumarate, unreacted monomers, and photo-initiator (AIBN) could no longer be detected by spectroscopic monitoring (Biotek UV–vis Spectrophotometer). Imprinted and control gels were then dried at room temperature for 24 h, followed by vacuum drying ($T = 30$ °C, 28 in. Hg vacuum) and then loaded with drug via equilibrium binding.

The ketotifen fumarate partition coefficient was calculated at equilibrium as

$$K_d = \frac{C_m}{C_e} = \frac{V_{sol}(C_i - C_e)}{V_{2,s}C_e} \quad (1)$$

where C_m is the concentration of solute within the gel, C_e is the concentration of ketotifen in solution after equilibrium has been reached, C_i is the initial concentration of ketotifen in solution (0.4 mg/mL), and V_{sol} and $V_{2,s}$ are the volumes of the solution and the swollen gel, respectively.

The aqueous solubility of ketotifen fumarate was measured by saturating ketotifen in deionized water, stirring overnight, adjusting the pH to a value of 7, and filtering. The concentration was measured by absorbance at 268 nm against a series of ketotifen standards.

The octanol/water partition coefficient ($\mathrm{Log}\,P_{octanol/water}$) was calculated as the logarithm of the ratio of the equilibrium concentrations of ketotifen in octanol to ketotifen in water. A 4 mL aliquot of a known concentration of aqueous ketotifen solution was shaken with 4 mL of octanol for 24 h and then let rest for 24 h. Concentration in octanol was obtained by mass balance.

3.3. Analysis of network swelling behavior and structural analysis of recognition

Equilibrium weight swelling studies were conducted under ambient conditions in both DI water and a concentrated ketotifen fumarate solution in DI water (0.5 mg/ml) on imprinted and control networks. Dynamic weight swelling ratios were plotted as a function of time until

Table 1
Characterization of transport in imprinted gels

Functional monomers (crosslinker)	Crosslinking amount (%), template, solvent	Characterization of binding parameters	Characterization of template transport	MIP structural/ swelling analysis	Reference
MAA (EGDMA)	• High (83%), histamine, acetonitrile • High (83%), ephedrine, chloroform • High (83%), theophylline, chloroform • High (83%), propranolol, chloroform	• Theophylline IPs bound 2× over NIPs • Discrimination and separation of enantiomers of propranolol and pindolol • Ephedrine and histamine chromatographic data show higher binding for templates	Propranolol permeates at slower rate with MIPs included in transdermal device than the controls	No	[24]
HEMA/MAA (EGDMA) HEMA/MMA (EGDMA)	Low (0.128%), timolol, no solvent	HEMA/MAA IPs bind 12 mg/g at pH 5.5, NIPs bind 4 mg/g. HEMA/MMA IPs demonstrate poor binding	90–100% release in 9 h	Yes (swelling)	[25]
HEMA/AA/AM/NVP (PEG200DMA)	Low (5%), ketotifen fumarate, no solvent	Most biomimetic IP (AA/AM/NVP/HEMA) bound 0.05 mmol/g, with NIP binding 0.008 mmol/g	Most biomimetic network released 65% in 3.5 days and 100% in 5 days	Yes (swelling)	[1]
MAA (EGDMA)	Weak, timolol, no solvent	IP demonstrated higher affinity than NIP	Drug diffusion coefficient from IP at certain M/T ratios (1/16, 1/32) 2 orders of magnitude lower than NIP	Yes (swelling)	[26]
MAA (EGDMA)	Moderate (57%), sulfasalzine, acetonitrile/ toluene (77/23 vol%)	None reported	IP particle release slower than NIPs. NIPs release 100% and MIPs release 80% in 5 h. Average IP and NIP particle sizes are different.	No	[27]
HEMA (EGDMA)	High (72.4%), cortisone, chloroform	• Testosterone (T) IP: 1.75 ± 0.04 μg/mg NIP: 0.36 ± 0.02 μg/mg • Hydrocortisone (H) MIP: 2.96 ± 0.05 μg/mg NIP: 0.46 ± 0.03 μg/mg	• Switch release in water of T triggered by H: 171 ± 3 μg (100% fractional release) in 4 h • Cumulative Release of T from MIP in Water: 61 ± 1 μg in 4 h (35% fractional release), 45% fractional release of T in 24 h	No	[28]
MAA (EGDMA)	High (50–90%), tetracycline	Range with highest (80% crosslinked) partition coefficient of 107.4 and 3.84 mg/g; IP partition coefficients 3–5 times higher than controls	IP shows slower release kinetics. However, only 20% released at 8 h with no further release	No	[29]
MAA (EGDMA)	High and moderate (77% & 44%), cholesterol, THF;THF/DMSO; THF/water; THF/water/ salt	Higher crosslinked structures had higher binding compared to NIP (maximum at 77% was ~13 times)	Transport of template into gel for up to 1500 min. IP had lag time in binding	Yes (swelling and structural analysis)	[30]
AM (EGDMA; PEGnDMA)	Variable (80%, 67%, 30%), glucose, DMSO	Binding of glucose analogue in water, tighter mesh-sized IP networks demonstrate increased affinity and capacity	No differences between IP and controls, different porosity and mesh structure affected release in water	Yes (swelling)	[31]
MAA (EGDMA)	High (82%), chloroform, theophylline	HPLC evaluation: template separation versus caffeine and capacity factors high for IP	IP release at various loading of Theophylline from 500 to 700 min at pH 7 (50% released from 50 to 200 min), NIP was both higher and lower at various pH values and loading	No	[32]

(*continued on next page*)

Table 1 (*continued*)

Functional monomers (crosslinker)	Crosslinking amount (%), template, solvent	Characterization of binding parameters	Characterization of template transport	MIP structural/ swelling analysis	Reference
MAA (EGDMA)	Low and high (79%, 81%); *R*- and *S*-ibuprofen, *R*- and *S*-ketoprofen, *R*- and *S*-propanol; toluene/water or chloroform or DMF	Partition coefficients of *R*- and *S*-propranolol into *S*-propranolol MIP are 1010 and 1790	• Release of eutomer from its imprinted polymer was faster than the distomer for high swelling gels. Reverse trend for low swelling gels.	Yes (swelling)	[33–36]
NAA (EGDMA)			• 100% of *S*-enantiomer (eutomer) released from *S*-imprinted polymer in 12 hrs as compared to 80% release of *R*-enantiomer (distomer)		
VPD (EGDMA)			• S-enantiomer permeates faster through *S*-imprinted polymer layered pore		

Crosslinking % is equivalent to (100% × (mole crosslinking monomer/(mole crosslinking monomer and all other monomers))).
Abbreviations: IP, imprinted polymer; NIP, non-imprinted polymer; MAA, methacrylic acid; EGDMA, ethylene glycol dimethacrylate; HEMA, 2-hydroxyethylmethacrylate; VPD, 4-vinylpyridine; AA, acrylic acid; AM, acrylamide; NVP, *N*-vinyl 2-pyrrolidinone; PEG200DMA, poly(ethylene glycol)200 dimethacrylate; MMA, methyl methacrylate; DMF, dimethylformamide; NAA, *N*-acryloyl-alanine polymer.

equilibrium. Weight swelling ratios at various times were obtained by the ratio of the swollen weight to the dry weight.

Each polymer sample was dried to a constant weight at ambient temperature under vacuum after washing ketotifen fumarate from the gel. Dry samples ($N' = 3$) were placed in a constant volume of deionized water with and without drug template at 25 °C. The gels were weighed by removing the gels from the swelling media at specific periods of time and blotting with absorbent, lint-free tissue to remove excess surface solvent. When the samples reached equilibrium water uptake, weight measurements were taken again by employing a buoyancy technique to determine sample volumes.

The equilibrium volume swelling ratio, Q, was calculated as follows:

$$Q = \frac{1}{\upsilon_{2,S}} = \frac{V_{2,S}}{V_{2,d}} \tag{2}$$

where $V_{2,S}$ is the swollen gel volume at equilibrium, $V_{2,d}$ is the volume of the dry polymer, and $\upsilon_{2,S}$ is the polymer volume fraction in the swollen state [13]. The volume of the gel in the swollen or dry state was obtained by using Archimedes buoyancy principle.

The average molecular weight between crosslinks, $\overline{M_C}$ was determined from the theory of rubber elasticity [14–16]. For an isotropic swollen hydrogel synthesized in the absence of solvent, with a constant deformation volume, Eq. (3) is valid for short elongation ratios of up to 2.

$$\tau = \left(\frac{RT\upsilon_{2,S}^{1/3}}{\bar{v}\overline{M_C}}\right)\left(1 - \frac{2\overline{M_C}}{\overline{M_N}}\right)\left(\alpha - \frac{1}{\alpha^2}\right) \tag{3}$$

where τ is the stress, α is the elongation ratio in any direction (final length/initial length), R is the universal gas constant, T is the absolute temperature, $\overline{M_N}$ is the number average molecular weight of the primary polymer chains prepared under identical conditions without crosslinking agent and $\bar{v}$ is the specific volume of the swollen polymer.

If $\overline{M_C} << \overline{M_N}$, which we confirmed, $\left(1 - \frac{2\overline{M_C}}{\overline{M_N}}\right) \to 1$, and Eq. (3) becomes,

$$\tau = \left(\frac{RT\upsilon_{2,S}^{1/3}}{\bar{v}\overline{M_C}}\right)\left(\alpha - \frac{1}{\alpha^2}\right) \tag{4}$$

Stress–strain data were obtained by performing tensile studies on a dynamic mechanical analyzer (TA Instruments, Wilmington, DE). Polymer gels were cut into thin sheets, clamped between the two parallel arms of the dynamic mechanical analyzer and subjected to a linear load. Strain values were converted into the elongation function $(\alpha - \frac{1}{\alpha^2})$ and the curves obtained had excellent correlation coefficients (>0.99). The slopes were used to calculate $\overline{M_C}$.

A structural parameter that is often used in describing the size of the network pores is the correlation length, ξ, which is defined as the linear distance between two adjacent crosslinks, and can be calculated using Eq. (5):

$$\xi = \alpha\sqrt{\bar{r}_0^2} \tag{5}$$

where $\sqrt{\bar{r}_0^2}$ is the root-mean-square, unperturbed, end-to-end distance of the polymer chains between two neighboring crosslinks. For isotropically swollen gels, the elongation ratio, α, is related to the swollen polymer volume fraction, using Eq. (6):

$$\alpha = \upsilon_{2,s}^{-1/3} \tag{6}$$

The unperturbed end-to-end distance of the polymer chain between two adjacent crosslinks can be calculated using the following equation,

$$\sqrt{\bar{r}_0^2} = l(C_n N)^{1/2} \tag{7}$$

where C_n is the Flory characteristic ratio, l is the length of the bond along the polymer backbone (which is equal to 1.54 Å for vinyl polymers), and N is the number of links/chain. The number of links per chain is equal to 2 times

the average molecular weight between crosslinks divided by the molecular weight of the repeating units from which the polymer chain is composed. Combining equations yields the correlation distance between two adjacent crosslinks in a swollen hydrogel

$$\xi = \upsilon_{2,s}^{-1/3}\left(\frac{2C_n\overline{M}_c}{M_r}\right)^{1/2} l \tag{8}$$

3.4. Experimental determination of diffusion coefficient

Ketotifen fumarate permeation studies through gels were conducted using Permegear side-by-side diffusion cells (Bethlehem, PA, USA) consisting of donor and receptor reservoirs. Water jackets around the reservoirs provided temperature control at 25 °C. Magnetic stirrers (600 rpm) in each reservoir kept the solutions well mixed.

A typical experiment for the determination of diffusional phenomena of ketotifen through hydrogel networks is as follows. Each gel was pre-swollen in deionized water (Millipore grade) until equilibrium. The swollen gels were placed between two half diffusion cells, and the receptor cell was filled with 3.1 mL of deionized water. Next the donor cell was filled with 3.1 mL of a 0.4 mg/mL ketotifen fumarate solution. At various time points, aliquots were taken from the receptor cell and the concentration of solute was measured. Each sample volume was replaced with an equivalent volume of water. From this experiment and applying Fick's first law in one-dimensional transport, the permeability coefficient, P, of the gel was determined. Corrected concentrations of solute in the receptor cell were calculated by accounting for the loss of solute due to the sampling technique. Also, the initial and end concentration of the donor side were compared to insure a relatively constant concentration driving force.

The diffusion coefficient of the solute in the gel, D, was then calculated by using the following equation:

$$D = \frac{P\delta}{K_d} \tag{9}$$

where K_d is the partition coefficient of the solute in the gel, and δ is the thickness of the swollen gel [17]. In order to determine the partition coefficient, thoroughly washed dry gels were placed in a solution containing a known concentration of solute, as described previously in Section 3.1.

4. Results and discussion

4.1. Equilibrium partitioning of ketotifen in gels

The partition coefficients for the imprinted networks, determined from equilibrium partitioning experiments, were 2 or more times greater than the control networks (Fig. 2a). Also, the partition coefficient of the (poly(AA-co-AM-co-NVP-co-HEMA-co-PEG200DMA)) network was measured as 45.05 as compared to 5.65, 7.13, and 5.31 for the single monomer networks poly(AA-co-HEMA-PEG200DMA), poly(AM-co-HEMA-PEG200DMA), and poly(NVP-co-HEMA-PEG200DMA), which is at least 8 times improvement in loading. These observations indicate that the imprinting technique results in structural plasticity of polymer chains, and is responsible for creating macromolecular memory due to the organization of multiple functionalities in the macromolecular architecture. Structural plasticity occurs in nature and an analogous situation is found in nervous systems. During a learning experience, reversible structural changes to synaptic morphology (such as remodeling of cytoskeletal and adhesion molecules, and AMPA receptor trafficking during long term potentiation and long term depression) result in modifications to synaptic transmission, and these changes are then stabilized for the creation of memory [18–20]. The imprinting process also involves structural changes, with the stabilization and constraining of polymer chain conformations by the template molecule, leading to the creation of memory sites. The octanol and water phase concentrations were calculated and checked by mass balance. The $\log_{10}$ octanol–water partition coefficient of ketotifen is -0.3, and it has an aqueous solubility of 3.4 mg/mL at pH 7 ± 0.2 and 25 °C. This indicates that the enhanced loading of the therapeutic is not due to hydrophobic interactions between the functional monomers and therapeutic, but rather due to the memory created by template-mediated constraints during polymerization.

4.2. Structural analysis of gels

We conducted dynamic penetrant studies in deionized water and 0.5 mg/ml concentrated ketotifen solution (data not statistically different for both cases). The equilibrium weight swelling ratios were similar for imprinted and control networks, which might suggest that similar macromolecular architectures are available for free volume transport. The gels in this work contain less than 1% monomers of ionic nature and are therefore considered neutral gels. Swelling studies at different pH values revealed no differences in swollen polymer volume fractions. A critical experimental parameter in the structural analysis of hydrogels, the swollen polymer volume fraction can be correlated with molecular parameters such as mesh size, average molecular weight between crosslinks and correlation length. There were no observable trends in the mesh sizes obtained from the tensile behavior of the gels. Comparable values were obtained for imprinted and non-imprinted gels, in the ranges of 21–31 Å (Fig. 2b). The Flory characteristic ratio was taken as 6.2 (an arithmetic mean of syndiotactic and isotactic poly(HEMA) networks) for these calculations [21]. The hydrodynamic radius of ketotifen fumarate is 4.2 Å, making it amenable to diffusion through the network. The average equilibrium polymer volume fraction in the swollen state was determined to be 0.634 ± 0.025 for the imprinted gels and was 0.645 ± 0.02 for the control gels (Fig. 2c and Table 2). These experimental results suggest that the structural plasticity due to imprinting, i.e.

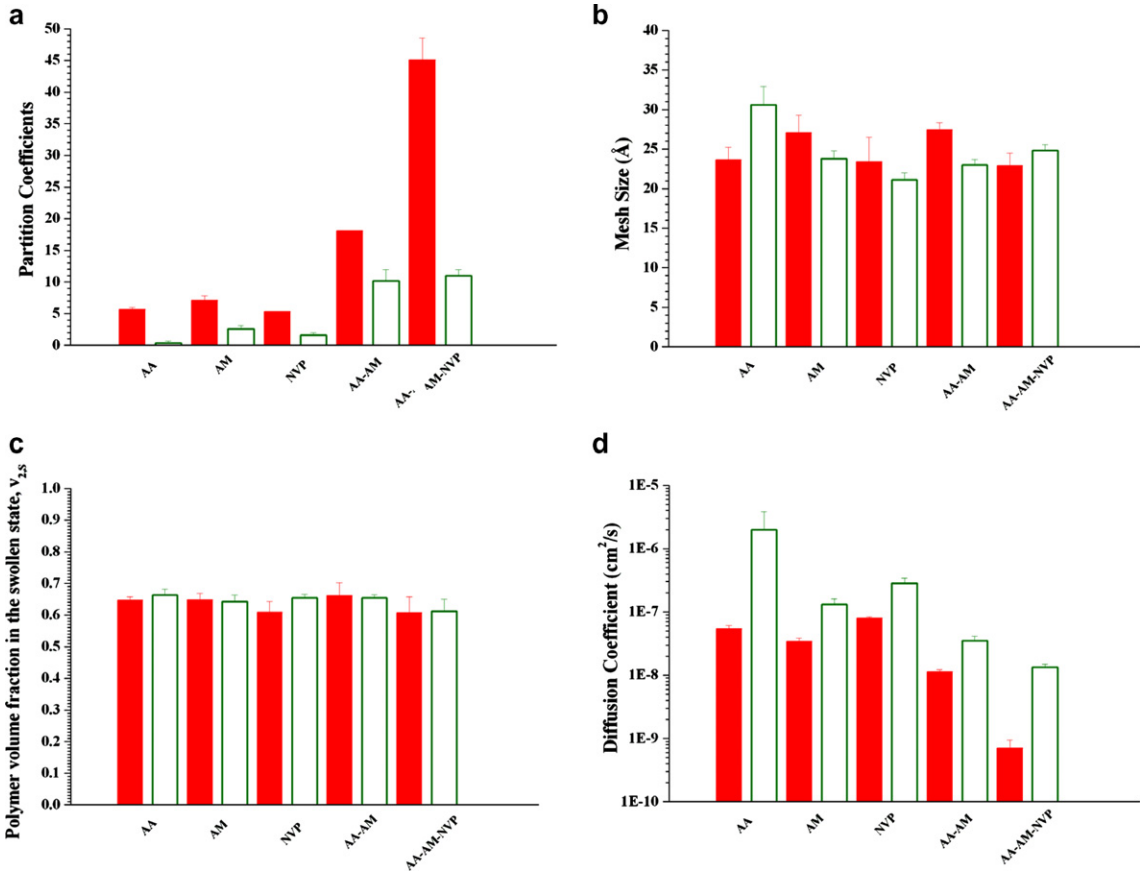

Fig. 2. (a) Partition coefficients, (b) mesh sizes obtained *via* tensile studies, (c) equilibrium polymer volume fractions in the swollen state, (d) diffusion coefficients obtained *via* permeation studies, for poly(*n*-co-HEMA-co-PEG200DMA) networks with a crosslinking percentage of 5 mole %. $N' = 3$, and T = 25 °C, where *n* is AA, AM, NVP, AA-co-AM, and AA-co-AM-co-NVP. Imprinted network (■) and Control network (□).

organization of multiple chemical functionalities is responsible for enhanced partitioning.

4.3. Experimental determination of diffusion coefficients: the "Tumbling Hypothesis"

Permeation studies conducted on the gels yielded a permeability coefficient of 7.98×10^{-7} cm/s for the imprinted (poly(AA-co-AM-co-NVP-co-HEMA-co-PEG200DMA)) network as compared to 4.34×10^{-6}, 3.5×10^{-6} and 6.06×10^{-6} cm/s (Table 2) for the single monomer imprinted networks, poly(AA-co-HEMA-PEG200DMA), poly(AM-co-HEMA-PEG200DMA), and poly(NVP-co-HEMA-PEG200DMA). Fig. 2d presents the ketotifen fumarate diffusion coefficients of all gel formulations studied. All imprinted networks had lower diffusion coefficients than non-imprinted networks in spite of comparable mesh sizes and equilibrium polymer volume fractions in the swollen state. The diffusion coefficient of the poly(AA-co-AM-co-NVP-co-HEMA-co-PEG200DMA)) network was 7.08×10^{-10} cm^2/s which was lesser by factors of 15, 76, 49 and 113 than the other imprinted networks (Table 2). We conclude that the multiplicity and organization of functionality are responsible in binding events and a delay in

Table 2
Transport coefficients and swelling data of poly(n-co-HEMA-co-PEG200DMA) networks

Network monomers (N)	Network type	Permeability *P* ($\times 10^6$ cm/s)	Diffusion coefficient ($\times 10^9$ cm^2/s)	$v_{2,S}$, Equilibrium polymer volume fraction in the swollen state	$\overline{M_C}$, Average molecular weight between crosslinks (g/mol)
AA	Imprinted	4.34 ± 0.51	53.68 ± 7.09	0.647 ± 0.011	1823 ± 244
	Control	9.87 ± 0.27	1988 ± 1860	0.664 ± 0.018	3109 ± 466
AM	Imprinted	3.5 ± 0.2	34.4 ± 4.08	0.648 ± 0.021	2502 ± 392
	Control	5.03 ± 0.12	132.1 ± 28.8	0.643 ± 0.020	1838 ± 153
NVP	Imprinted	6.06 ± 0.24	79.92 ± 4.03	0.608 ± 0.034	1728 ± 452
	Control	6.52 ± 0.15	281.7 ± 58.2	0.654 ± 0.012	1481 ± 121
AA-co-AM	Imprinted	2.92 ± 0.21	11.33 ± 0.88	0.661 ± 0.041	2494 ± 123
	Control	5.11 ± 0.28	35.11 ± 6.44	0.654 ± 0.010	1736 ± 102
AA-co-AM-co-NVP	Imprinted	0.8 ± 0.2	0.708 ± 0.236	0.608 ± 0.049	1647 ± 211
	Control	3.65 ± 0.24	13.31 ± 1.62	0.612 ± 0.038	1948 ± 83

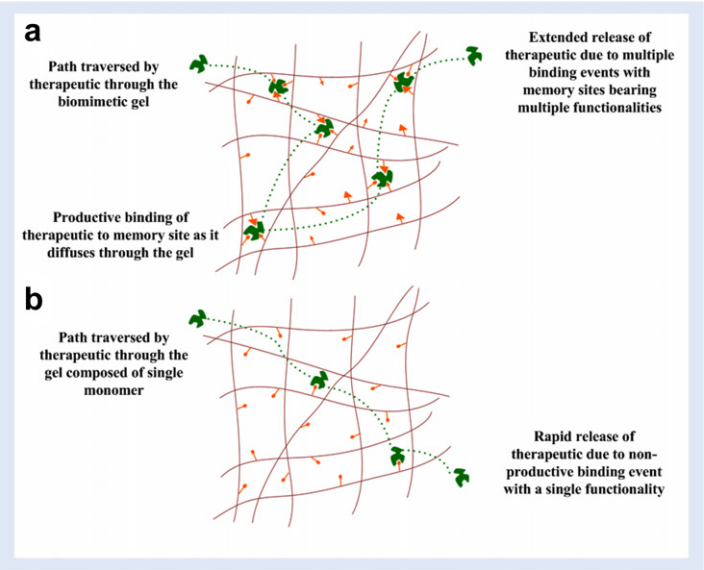

Fig. 3. (a) Tumbling of the drug through the gel from one memory site to the next results in slower diffusion coefficients and delayed kinetics of release. This could be imputed to productive binding of the drug at every memory site a drug molecule encounters due to multiple contact points. (b) Single monomer gels have single contact points and have less effective binding events with the drug, resulting in rapid release. Dotted lines ····· indicate the pathway of diffusion through the gel in both cases.

transport. The imprinted networks of all the gels studied had lower permeability and diffusion coefficients than the control networks, demonstrating that imprinting does delay transport. It is expected that the phenomenon of enhanced loading and extended release would be significantly reduced upon increasing the mesh size, which would affect the organization of functional groups interacting with the template.

We propose that as a molecule makes its random walk through a network imprinted by it, it tumbles from one memory site to the next, where it is held by the complex hydrogen bonding patterns, thus increasing its mean residence time in the network (Fig. 3). There are greater and more productive binding events in a recognitive network composed of multiple functional monomers than in non-imprinted control networks and networks composed of single functional monomers. A control network is not constrained to polymerize around the template during polymerization and hence possesses no macromolecular memory. Gels composed of single functional monomers do not have multiple contact points with the drug to bind to it for a longer duration. These molecular binding events are translated into extended release and lower diffusion coefficients.

The "tumbling hypothesis" is supported by earlier thermodynamic theories of imprinting processes. The free energy of functional monomer–template complex formation in the pre-polymerization complex and the stability of the complex are a function of the extent of favorable non-covalent interactions and determine the fidelity of memory sites [22,23]. Functionally diverse systems are capable of multiple contact points with the template molecule, and result in efficient template complexation due to the reduction in the entropically unfavorable translational and rotational free energies. The poly(AA-co-AM-co-NVP-co-HEMA-co-PEG200DMA)) network can form multiple favorable non-covalent interactions with the template molecule, as it tumbles through the network. The functional monomer–template binding is not tight enough to preclude the unbinding event.

Furthermore, the polymer volume fraction in the swollen state for the poly(AA-co-AM-co-NVP-co-HEMA-co-PEG200DMA)) network was observed to be slightly less than the other networks, which could mean a more open network available for free volume transport. In spite of this, the drug does not diffuse through faster, but is delayed compared to all the other systems due to the tumbling from one memory site to the next.

5. Conclusions

We have shown that imprinting a network results in macromolecular memory for the template molecule, indicated by the two or more times greater partitioning into these networks as compared to non-imprinted networks. Partitioning of drug into the poly(AA-co-AM-co-NVP-co-HEMA-co-PEG200DMA) network was 8 times greater than networks synthesized from single monomers. The equilibrium polymer volume fractions in the swollen state and mesh sizes were comparable for all the imprinted and control gels studied, indicating that the macromolecular structures were similar. On the other hand, all imprinted networks had lower diffusion coefficients than non-imprinted networks, with the most diverse functionalized networks displaying significantly delayed transport. Hence, the organization of the chemical functionality plays a

major role in enhanced partitioning and delayed transport. This could be interpreted in terms of heightened interactions of the template molecule with memory sites while it is diffusing through the network. Such imprinted networks hold immense potential in the fields of drug delivery and nanobiotechnology.

Acknowledgments

We thank Dr. Mirna Mosiewicki De Ruiz and Dr. Maria Lujan Auad (Department of Polymer and Fiber Engineering, Auburn University) for aiding with the tensile studies. We thank Maryam Ali for the ketotifen octanol/water partition coefficient and solubility data and Efe Sahinoglu for permeation studies on the poly(AA-co-AM-co-NVP-co-HEMA-co-PEG200DMA) network. This research was supported by the National Science Foundation (NSF-EEC-0552557, Grant G00002215, S.H.P. was an NSF REU Fellow) and an Auburn University Biogrant.

References

[1] S. Venkatesh, S.P. Sizemore, M.E. Byrne, Biomimetic hydrogels for enhanced loading and extended release of ocular therapeutics, Biomaterials 28 (2007) 717–724.
[2] N.A. Peppas, Hydrogels in Medicine and Pharmacy, CRC Press, Boca Raton, FL, 1987, p 195.
[3] N.A. Peppas, P. Bures, W. Leobandung, H. Ichikawa, Hydrogels in pharmaceutical formulations, Eur. J. Pharm. Biopharm. 50 (2000) 27–46.
[4] K. Tahara, K. Yamamoto, T. Nishihata, Overall mechanism behind matrix sustained-release tablets prepared with hydroxypropyl methyl cellulose 2910, J. Control. Release 35 (1995) 59–66.
[5] E.S. Lee, S.W. Kim, S.H. Kim, J.R. Cardinal, H. Jacobs, Drug release from hydrogel devices with rate-controlling barriers, J. Membr. Sci. 7 (1980) 293–303.
[6] P.I. Lee, Novel approach to zero-order drug delivery via immobilized nonuniform drug distribution in glassy hydrogels, J. Pharm. Sci. 73 (1984) 1344–1347.
[7] G. Wulff, Molecular imprinting in crosslinked materials with the aid of molecular templates – a way towards artificial antibodies, Angew. Chem. Int. Ed. Engl. 34 (1995) 1812–1832.
[8] B. Sellergren, Noncovalent molecular imprinting: antibody-like molecular recognition in polymeric network materials, Trends Anal. Chem. 16 (1997) 310–320.
[9] M.E. Byrne, K. Park, N.A. Peppas, Molecular imprinting within hydrogels, Adv. Drug Del. Rev. 54 (2002) 149–161.
[10] C. Alvarez-Lorenzo, A. Concheiro, Molecularly imprinted polymers for drug delivery, J. Chromatogr. B: Anal. Tech. Biomed. Life Sci. 804 (2004) 231–245.
[11] J.Z. Hilt, M.E. Byrne, Configurational biomimesis in drug delivery: molecular imprinting of biologically significant molecules, Adv. Drug Deliver. Rev. 56 (2004) 1599–1620.
[12] M. Bruysters, A. Jongejan, M. Gillard, F. van de Manakker, R.A. Bakker, P. Chatelain, R. Leurs, Pharmacological differences between human and guinea pig histamine H1 receptors: Asn84 (2.61) as key residue within an additional binding pocket in the H1 receptor, Mol. Pharmacol. 67 (2005) 1045–1052.
[13] B. Kim, N.A. Peppas, Synthesis and characterization of pH-sensitive glycopolymers for oral drug delivery systems, J. Biomater. Sci. Polym. Ed. 13 (2002) 1271–1281.
[14] P.J. Flory, Principles of Polymer Chemistry, Cornell University Press, Ithaca, NY, 1953, p 672.
[15] P.J. Flory, J. Rehner Jr., Statistical mechanics of cross-linked polymer networks. II. Swelling, J. Chem. Phys. 11 (1943) 521–526.
[16] P.J. Flory, J. Rehner Jr., Statistical mechanics of cross-linked polymer networks. I. Rubberlike elasticity, J. Chem. Phys. 11 (1943) 512–520.
[17] H.J. Moynihan, M.S. Honey, N.A. Peppas, Solute diffusion in swollen membranes. Part V: solute diffusion in poly(2-hydroxyethyl methacrylate), Polym. Eng. Sci. 26 (1986) 1180–1185.
[18] T.H. Brown, J.H. Byrne, K.S. LaBar, J.E. LeDoux, D.H. Lindquist, R.F. Thompson, T.J. Teyler, Learning and memory: basic mechanisms, From Molecules to Networks, 2004, pp. 499–574.
[19] R. Lamprecht, J. LeDoux, Structural plasticity and memory, Nat. Rev. Neurosci. 5 (2004) 45–54.
[20] N.C. Tronson, J.R. Taylor, Molecular mechanisms of memory reconsolidation, Nat. Rev. Neurosci. 8 (2007) 262–275.
[21] J.H. Yoon, J.M. Shin, Y.K. Kang, M.S. Jhon, Conformational analysis of poly(2-hydroxyethyl methacrylate), J. Polym. Sci. Part A: Polym. Chem. 29 (1991) 393–398.
[22] I.A. Nicholls, K. Adbo, H.S. Andersson, P.O. Andersson, J. Ankarloo, J. Hedin-Dahlstrom, P. Jokela, J.G. Karlsson, L. Olofsson, J. Rosengren, S. Shoravi, J. Svenson, S. Wikman, Can we rationally design molecularly imprinted polymers? Anal. Chim. Acta 435 (2001) 9–18.
[23] I.A. Nicholls, Towards the rational design of molecularly imprinted polymers , J. Mol. Recognit. 11 (1998) 79–82.
[24] C.J. Allender, C. Richardson, B. Woodhouse, C.M. Heard, K.R. Brain, Pharmaceutical applications for molecularly imprinted polymers, Int. J. Pharm. 195 (2000) 39–43.
[25] C. Alvarez-Lorenzo, H. Hiratani, J.L. Gomez-Amoza, R. Martinez-Pacheco, C. Souto, A. Concheiro, Soft contact lenses capable of sustained delivery of timolol, J. Pharm. Sci. 91 (2002) 2182–2192.
[26] H. Hiratani, Y. Mizutani, C. Alvarez-Lorenzo, Controlling drug release from imprinted hydrogels by modifying the characteristics of the imprinted cavities, Macromol. Biosci. 5 (2005) 728–733.
[27] F. Puoci, F. Iemma, R. Muzzalupo, U.G. Spizzirri, S. Trombino, R. Cassano, N. Picci, Spherical molecularly imprinted polymers (SMIPs) via a novel precipitation polymerization in the controlled delivery of sulfasalazine, Macromol. Biosci. 4 (2004) 22–26.
[28] K. Sreenivasan, On the applicability of molecularly imprinted poly(HEMA) as a template responsive release system, J. Appl. Polym. Sci. 71 (1999) 1819–1821.
[29] W. Cai, R.B. Gupta, Molecular-imprinted polymers selective for tetracycline binding, Sep. Purif. Methods 35 (2004) 215–221.
[30] U.G. Spizzirri, N.A. Peppas, Structural analysis and diffusional behavior of molecularly imprinted polymer networks for cholesterol recognition, Chem. Mater. 17 (2005) 6719–6727.
[31] M.E. Byrne, J.Z. Hilt, N.A. Peppas, Recognitive biomimetic networks with moiety imprinting for intelligent drug delivery, J. Biomed. Mat. Res. Part A. 84A (2007) 137–147.
[32] M.C. Norell, H.S. Andersson, I.A. Nicholls, Theophylline molecularly imprinted polymer dissociation kinetics: a novel sustained release drug dosage mechanism, J. Mol. Recognit. 11 (1998) 98–102.
[33] R. Suedee, T. Srichana, R. Chotivatesin, G.P. Martin, Stereoselective release behaviors of imprinted bead matrices, Drug Dev. Ind. Pharm. 28 (2002) 545–554.
[34] R. Suedee, T. Srichana, G.P. Martin, Evaluation of matrices containing molecularly imprinted polymers in the enantioselective-controlled delivery of beta-blockers, J. Control. Release 66 (2000) 135–147.
[35] R. Suedee, T. Srichana, T. Rattananont, Enantioselective release of controlled delivery granules based on molecularly imprinted polymers, Drug Deliv. 9 (2002) 19–30.
[36] C. Bodhibukkana, T. Srichana, S. Kaewnopparat, N. Tangthong, P. Bouking, G.P. Martin, R. Suedee, Composite membrane of bacterially-derived cellulose and molecularly imprinted polymer for use as a transdermal enantioselective controlled-release system of racemic propranolol, J. Control. Release 113 (2006) 43–56.